Accepted Manuscript

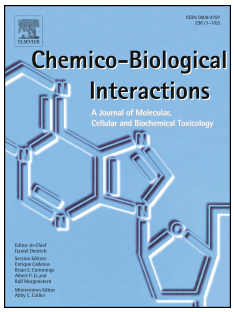

Biological activity of a small molecule indole analog, 1-[(1H-indol-3-yl)methylene]-2-phenylhydrazine (HMPH), in chronic inflammation

Chandra Sekhar Misra, G.H. Chethan, Srinivas Reddy Jitta, Karthik Gourishetti, Prasanthi Daram, Mahendra Pal Singh, H.S. Akhila, Yogendra Nayak, Mazhuvancherry Keshavan Unnikrishnan, Dr. Professor and Head, Department of Pharmacy Practice

PII: S0009-2797(15)30101-0

DOI: 10.1016/j.cbi.2015.10.024

Reference: CBI 7507

To appear in: *Chemico-Biological Interactions*

Received Date: 1 August 2015

Revised Date: 15 October 2015

Accepted Date: 31 October 2015

Please cite this article as: C.S. Misra, G.H. Chethan S.R. Jitta, K. Gourishetti, P. Daram, M.P. Singh, H.S. Akhila, Y. Nayak, M.K. Unnikrishnan, Biological activity of a small molecule indole analog, 1-[(1H-indol-3-yl)methylene]-2-phenylhydrazine (HMPH), in chronic inflammation, *Chemico-Biological Interactions* (2015), doi: 10.1016/j.cbi.2015.10.024.

Biological activity of a small molecule indole analog, 1-[(1H-indol-3-yl)methylene]-2-phenylhydrazine (HMPH), in chronic inflammation

Chandra Sekhar Misra[a], Chethan G. H.[a], Srinivas Reddy Jitta[b], Karthik Gourishetti[c], Prasanthi Daram[b], Mahendra Pal Singh[d], Akhila H.S.[a], Yogendra Nayak[c], Mazhuvancherry Keshavan Unnikrishnan[a,*]

[a]Department of Pharmacy Practice, [b]Department of Pharmacognosy, [c]Department of Pharmacology, Manipal College of Pharmaceutical Sciences, Manipal University, Karnataka, Manipal – 576104, India.

[d]Department of Pharmacology, Life Science Research Centre in India, Daiichi Sankyo India Pharma Private Limited, Gurgaon – 122015, India.

*** Corresponding Author:**

Dr. Mazhuvancherry Keshavan Unnikrishnan,

Professor and Head, Department of Pharmacy Practice,

Manipal College of Pharmaceutical Sciences, Manipal University,

Manipal – 576104, Karnataka, India.

Phone: +91 820 2922482, Fax: +91 820 2571998,

E-mail: mkunnikrishnan@gmail.com

Graphical Abstract:

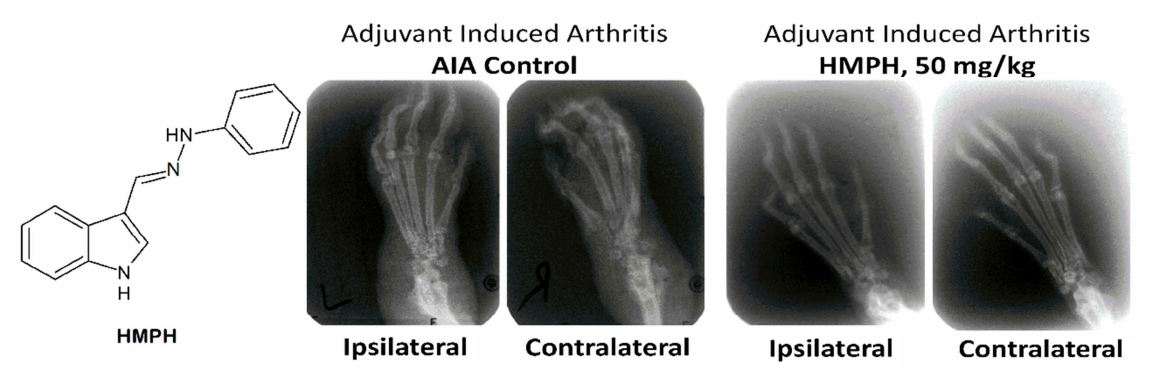

Highlights:

- HMPH scavenged free radicals and protected the lipid membrane.
- Reduced the LPS-induced ROS/nitrite and TNF-α release in *in vitro* assays.
- Inhibited MPO, nitrite and leucocyte infiltration in inflammatory rat models.
- Protected bone deformation and reduced acute and chronic inflammation.
- Acts as an immunomodulator and inhibited TNF-α.

Abstract

A synthetic small molecule, 1-[(1*H*-indol-3-yl)methylene]-2-phenylhydrazine (HMPH) was conveniently synthesised by a one-step reaction, purified and characterised by chromatographic and spectroscopic methods. HMPH scavenged free radicals and inhibited lipopolysaccharide (LPS)-induced ROS generation and NO release in RAW-264.7 cells without signs of any detectable cytotoxicity. HMPH inhibited lipid peroxidation (LPO) with IC_{50} of 135 ± 9 as against 58 ± 8 µM for α-tocopherol. Further, HMPH (>50 µM) significantly reduced the LPS-induced TNF-α release in mouse peritoneal macrophages and in human peripheral blood mononuclear cells (PBMCs). HMPH did not show any visible signs of toxicity in rats up to 400 mg/kg/intraperitoneal and 2000 mg/kg/oral. HMPH at 25 and 50 mg/kg attenuated neutrophil infiltration in air-pouch lavage and bronchoalveolar lavage (BAL) in rat models. HMPH also reduced myeloperoxidase (MPO), nitrite and TNF-α in air-pouch lavage in addition to MPO in plasma. HMPH reduced acute paw-inflammation in carrageenan-induced paw-edema. HMPH consistently decreased both ipsilateral and contralateral paw inflammation, minimised the clinical scores of arthritis, prevented body weight (B.wt.) loss, attenuated serum C-reactive protein (C-RP) and rheumatoid factors (RF) in rat model of adjuvant-induced arthritis. Histopathology and radio-graphical reports show that HMPH reduced bone erosion in both ipsilateral and contralateral paw joints. Failure to inhibit COX suggests that effectiveness of HMPH in both acute and chronic inflammation is mediated by a multimodal mechanism involving modulation of immunity, attenuating TNF-α, protecting bone attrition and reducing oxidative stress.

Keywords:
Anti-inflammatory
HMPH [1-((1H-indol-3-yl) methylene)-2-phenylhydrazine]
Carrageenan
Lipopolysaccharide
TNF-α
Arthritis

Abbreviations:

ABTS, 2, 2'-azino-bis-(3-ethylbenzothiazoline-6-sulphonic acid);AIA, adjuvant induced arthritis; AMPK, 5'-adenosine monophosphate-activated protein kinase; BAL, bronchoalveolar lavage; CFA, complete Freund's adjuvant; CMC, carboxymethyl cellulose; COX, cyclooxygenase; C-RP, C-reactive protein; DHPO, 1-oxo-2-(2H-pyrroliun-1-yl)-1H-inden-3-olate, AMPK signalling activator; Diclo 10, diclofenac 10 mg/kg; DMEM, Dulbecco's modified Eagle's medium; DPI, diphenyleneiodonium; DPPH, 2, 2-diphenyl-1-picrylhydrazyl; ELISA, enzyme-linked immune-sorbent assay; FBS, fetal bovine serum; HBSS, Hanks' balanced salt solution; HMPH 12.5, HMPH 12.5 mg/kg; HMPH 25, HMPH 25 mg/kg; HMPH 50, HMPH 50 mg/kg; IL, interleukins; iNOS, inducible NOS (nitric oxide synthase); $_{L}$-NAME, $_{L}$-N^{G}-nitroarginine methyl ester; LOX, lipoxygenase; LPO, lipid peroxidation; LPS, lipopolysaccharides; MDA, malondialdehyde; MPO, myeloperoxidase; MTT, 3-(4, 5-dimethylthiazol-2-yl)-2, 5-diphenyltetrazolium bromide; NSAIDS, non-steroidal anti-inflammatory drugs; OECD, organisation for economic co-operation and development; PBMCs, peripheral blood mononuclear cells; PG, prostaglandin; RF, rheumatoid factor; ROS, reactive oxygen species; SEM, standard error mean; TBARS, thiobarbituric acid reactive substances; TLR-4, toll like receptor-4; TNF-α, tumour necrosis factor alfa; WBC, white blood cells.

1. Introduction

Inflammatory responses address a wide variety of noxious stimuli such as infections, antigens and physical/chemical injuries. NSAIDs are among the most prominent class of anti-inflammatory drugs, chiefly acting via COX inhibition with antipyretic, analgesic and anti-inflammatory actions [1]. On the other hand, the parallel inhibition of COX-1 largely accounts for undesirable effects such as gastro-intestinal ulcers (GI ulcers) [2]. COX-2 specific inhibitors like celecoxib reduces the risk of GI ulcer but result in cardiovascular adverse events [3]. Aspirin irreversibly acetylates COX, whereas the propionic acid derivatives (ibuprofen, naproxen etc.), acetic acid derivatives (ketorolac, diclofenac etc.), enolic acids (piroxicam) and fenamic acids (mefenamic acid) compete reversibly with the arachidonic acid at the active site of COX-1 and COX-2 [4]. Apart from COXs, histamine, serotonin, bradykinin, leukotrienes (LTs) and the platelet activating factors (PAFs) participate in the inflammatory process [5, 6]. Pro-inflammatory LTs aggravate asthma and LT-receptor antagonists (montelukast and zafirlukast) attenuate asthma symptoms [7].

Cytokines such as TNF and interleukins (IL) [5] also orchestrate chronic inflammation. TNF-α blockers treat chronic inflammatory conditions, including rheumatoid arthritis (RA), juvenile idiopathic arthritis, psoriasis and psoriatic arthritis, ankylosing spondylitis, and Crohn's disease [6]. RA is an autoimmune disease driven largely by activated T cells, producing T cell–derived cytokines such as IL-1 and TNF-α. The human recombinant IL-1 receptor antagonist (IL-1ra; anakinra) inhibits structural damage in RA [8]. TNF-α blockers (infliximab, etanercept etc.) are disease-modifying anti-rheumatic drugs (DMARDs) [9].

Indole derivatives have been widely screened for anti-inflammatory activity via AMPK activation [10, 11] and inhibition of multiple pathways in inflammation [12]. Our research group has reported dual COX-LOX inhibitors with anti-inflammatory activity; E.g.

1-oxo-2-(2H-pyrrolium-1-yl)-1H-indene-3-olate, DHPO, with anti-oxidant, free radical scavenger activity and AMPK activating ability [13, 14]. Similar compounds were later reported to be anti-inflammatory through inhibition of NF-κB and IL-6 pathways [15]. HMPH, the subject of this paper, also showed a non-COX mediated mechanism of action via TNF-α inhibition and immune modulating potential in both acute and chronic models of inflammation.

2. Materials and Methods

2.1. Materials

Indole-3-carboxaldehyde, phenyl hydrazine, 2,2-diphenyl-1-picrylhydrazyl (DPPH), 2,2-azino-bis-(3-ethylbenzothiazoline-6-sulphonic acid) or ABTS, Lipopolysaccharide from *Escherichia coli* 0111:B4 (LPS, Cat# L4391), Ficoll Histopaque (Cat# 10771), Ortho dianisidine hydrochloride, 2,7-dichlorofluorescein diacetate (DCFH-DA), Diphenylene iodonium (DPI), Nω-nitro-L-arginine methyl ester hydrochloride (L-NAME hydrochloride), λ- carrageenan, INF-γ and Dulbecco's modified Eagle's medium (DMEM, Cat# D-7777) were purchased from Sigma-Aldrich Co., USA. 3-(4,5-dimethylthiazol-2-yl)-2,5-diphenyl tertrazolium bromide or MTT procured from HiMedia Laboratories, Mumbai, India, Foetal Bovine Serum (FBS) was obtained from Invitrogen BioServices India Pvt. Ltd., Bengaluru, India (Gibco® Cat# 10270), Heparinized vacutainer from BD India Pvt. Ltd., Bengaluru, India (Cat# 367671), Tissue culture accessories were procured from Greiner Bio-One GmbH, Frickenhausen, Germany. All other chemicals or reagents purchased were of analytical grade. Diclofenac sodium was obtained as a gift sample from Hetero Drugs Ltd., Hyderabad, India.

2.2. Methods

2.2.1. Synthesis, characterization, purity assessment and molecular property prediction

2.2.1.1 Procedure for Synthesis of HMPH. HMPH was synthesized by a convenient one-step reaction. (Fig. 1). Briefly, equimolar quantities of indole-3-carboxaldehyde (**1**) and phenyl hydrazine (**2**) were dissolved in ethanol, refluxed for 2 h in presence of glacial acetic acid

(catalyst), cooled, filtered, washed with cold ethanol, recrystallized from ethanol and dried, to yield 1-((1H-indol-3-yl)methylene)-2-phenylhydrazine (HMPH; **3**) with high purity.

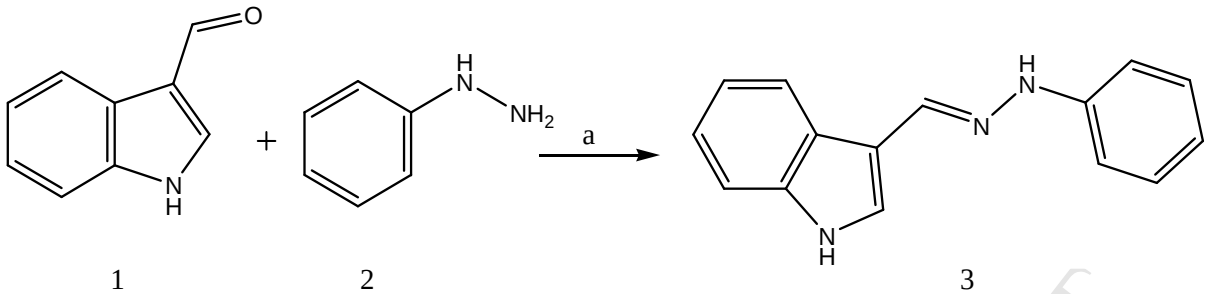

1 2 3

Fig. 1. Synthetic pathway of HMPH; [a]Ethanol, glacial acetic acid, reflux, 2 h.

2.2.1.2 Characterization and purity assessment. Reaction was monitored by thin layer chromatography (Merck Silica Gel 60 F254 TLC plates) and detected by UV light (λ= 254 nm)/iodine vapors. Melting point was determined and FT-IR spectrum was recorded on Shimadzu FT-IR 8300 IR-spectrophotometer between 4000-400 cm^{-1}. Proton nuclear magnetic resonance spectroscopy (1H NMR) was recorded on a Bruker Ascend 400 MHz spectrometer (Internal standard: Tetramethylsilane). Mass spectrum (MS) was recorded using electrospray ionization (ESI) source and m/z ratio was reported.

The analytical purity of HMPH (1 mg/ml) was assessed by HPLC system equipped with dual pump LC-20AD binary system, photodiode array (PDA) detector SPD-M20A at 320 nm (Shimadzu Corporation, Japan), Merck C_{18} reverse-phase, operating at a flow rate of 1.0 ml/min and injection volume of 20 µl. Two pump linear gradient programs were employed; pump A - 0.1 % formic acid in water (v/v) and pump B - acetonitrile. Initially, a gradient elution from 10 % of B changing to 70 % was run for 25 min followed by 10 % of B for an additional 10 min. Purity of HMPH was established from the chomatographic peak and retention time (t_r). Physical and spectral properties of HMPH: Brown crystals; Yield-67.00 %; R_f - 0.85; m.p. 155 -156 °C; FT-IR:(KBr, Vmax): 3365 cm^{-1} (NH stretching) and 1630 cm^{-1} imine (C=N) linkage;^{1}H NMR: (400 MHz, DMSO-*d*6): δ (ppm); 6.64 (t, 1H), 7.01 (d, 2H), 7.12 (m, 4H), 7.39 (d, 1H), 7.60 (s, 1H), 8.10 (s, 1H, azomethine-CH), 8.23 (d, 1H), 9.79 (s,

1H, NH-hydrazine) 11.29 (s, 1H, NH-indole); MS-ESI: m/z 235; HPLC purity: > 99 %; retention time (t_r) = 26.81 min.

2.2.1.3. Prediction of molecular properties: The molecular properties of HMPH were predicted by a free online tool "Calculation of Molecular Properties" Molinspiration cheminformatics (www.molinspiration.com) and are summarized in Table 1.

Table 1

Predicted Molecular Properties of HMPH.

Compound	Molecular Weight	miLogP	n-rotb[a]	n-OHNH[b]	n-ON[c]	Lipinski's Violation
Lipinski's Rule	≤ 500	≤ 5	≤ 5	≤ 5	≤ 10	≤ 1
HMPH	235	4.914	3	2	3	0

[a]n-rotb - number of rotatable bonds; [b]n-OHNH - number of hydrogen bond donors; [c]n-ON - number of hydrogen bond acceptors.

Further, we investigated HMPH for its effect against inflammation by *in vitro* and *in vivo* methods.

2.2.2. In vitro screening assays

2.2.2.1. Cell culture maintenance. The murine macrophages (RAW 264.7) purchased from National Centre for Cell Science (NCCS), Pune, India was maintained in DMEM culture medium containing 10 % FBS and 1 % penicillin-streptomycin, at 37 °C in 95 % air and 5 % CO_2 in CO_2 incubator (NU-5510E, NuAire Inc., USA).

2.2.2.2. Cytotoxicity assay. HMPH was tested for cytotoxicity by MTT assay as reported earlier [16] with slight modifications. Briefly, RAW 264.7 cells were seeded (5×10^4 cells/well) in a sterile clear flat-bottom 96-well plate and was treated with HMPH (from 7.8 to 1000 µM) for 24 h. MTT reagent (50 µl, 1 mg/ml in sterile PBS, pH 7.4) was then added to all wells except blank and incubated for 4 h. The purple formazan dye generated by mitochondrial dehydrogenase (only in live cells) was dissolved by adding 100 µl of 100 %

DMSO to wells, mixed on a plate-shaker for 10 min and absorbance measured (λ= 540 nm) using microplate reader (ELx800, BioTek Instruments Inc., USA). The percentage viability was calculated [formula: ((absorbance of test compound – absorbance of blank)/(absorbance of MTT control – absorbance of blank))×100].

2.2.2.3. Reactive oxygen species (ROS) and nitrite inhibition assay. The assay was performed in RAW 264.7 murine macrophages by reported methods with slight modifications [15]. Cells were seeded (5×10^4 cells/well) in a sterile black flat-bottom 96-well plate. After 24 h, cells were treated with HMPH (0.5 to 500 µM) and reference standard (L-NAME 100 µM for nitrite and DPI 5 µM for ROS inhibition respectively) in triplicates. Two hours after incubation, cells were challenged with LPS 10 µg/ml (except blank wells) for 20 h, supernatant collected in a sterile clear flat-bottom 96-well plate for nitrite estimation using Griess reagent. Intracellular ROS was estimated by adding 100 µM of DCFH-DA to wells of black well plate, incubated for 1 h, washed once with sterile HBSS and the fluorescence was measured using microplate reader (FLx800, BioTek Instrument Inc., USA) at excitation λ= 485 nm and emission λ= 530 nm.

2.2.2.4. Free radical scavenging activity. Stable radicals DPPH and ABTS were employed for the assay [14]. Methanolic solution of HMPH (4 to 500 µM) was added to 100 µM DPPH methanolic solution, incubated in dark for 20 min at room temperature. DPPH reacts with electron-donating molecules (test/standard compounds) forming a colorless 2, 2'-diphenyl-1-picrylhydrazine, with absorbance (at λ= 517 nm) decreasing in proportion to activity.

Methanolic solutions of HMPH (4 to 500 µM) were incubated with 100 µM ABTS [prepared from 2 mM ABTS and 0.17 mM potassium persulfate in 20 mM phosphate buffer of pH 7.4] at room temperature for 10 min in dark. Absorbance was measured (λ= 734 nm) with curcumin as reference standard in both DPPH and ABTS assays. The experiment was performed in triplicates and IC_{50} were calculated.

2.2.2.5. Lipid peroxidation assay. Healthy rat brain was isolated and 10 % w/v homogenate was prepared in ice cold 1.15 % KCl, centrifuged (14000 rpm/10 min/4 °C), 200 µl of supernatant mixed with 400 µl of freshly prepared ferrous sulphate (2 Mm) in presence or absence of test/standard and incubated at 37 °C for 30 min. Reaction was stopped by adding 800 µl of ice cold TBA-TCA reagent (0.375 % w/v of TBA, 15 % w/v of TCA and 200 µl of 0.25 N HCl). The resulting mixture was heated at 80 °C for 30 min in water bath and pink chromogen was formed by TBA and malondialdehyde (MDA) reaction. Reaction mixture was cooled, centrifuged (5000 × g at 4 °C, 10 min) and supernatant plated (100 µl each) in triplicate into 96-well plate and absorbance (λ= 540 nm) read on a plate reader [17]. Inhibition of iron-induced LPO by HMPH and α-tocopherol (as reference standard) are expressed as IC_{50} values.

2.2.2.6. COX enzyme inhibition assay. HMPH at 0.25, 2.5, 25 and 250 µM, in methanol, was tested for COX-2 inhibition by following manufacturer's instructions (COX colorimetric inhibitor screening assay kit, Cayman Chemical, Cat# 701050).

2.2.2.7. TNF-estimation in mouse peritoneal macrophages. Monolayers of macrophages were prepared according to published method with brief modifications [18]. Peritoneal exudate cells (PEC) harvested from peritoneal lavage with 5 ml aliquots of chilled incomplete medium were transferred to 96 well plates (2×10^5 cells/ 200 µl/well) and incubated at 37 °C for 2 h in humidified CO_2 incubator. Non-adherent cells were removed by vacuum aspiration, and adherent cells were washed three times with warm serum-free medium and incubated overnight in complete medium for allowing macrophages to spread, then primed with 150 U/ml IFN-γ for 12 h and inoculated with HMPH (25, 50, 100 and 200 µM), with or without

LPS (10 ng/ml) for 24 h at 37 °C in 5% CO_2 incubator. LPS-induced TNF-α release was estimated by ELISA as per manufacturer's instructions (eBioscience, Cat# 88-7324-88).

2.2.2.8. TNF-α estimation in human peripheral blood mononuclear cells (PBMCs). Peripheral blood, withdrawn in a heparinized vacutainer from a healthy human volunteer was subject to gradient centrifuge (30 min at 100 × g/4 °C) in a swing-out bucket over Ficoll Histopaque [19]. Whitish buffy coat was aspirated and washed twice with sterile DMEM containing 1 % penicillin-streptomycin-amphotericin-B solution. PBMCs were re-suspended at 2.5×10^6 per ml in DMEM containing 10 % FBS and were incubated (2.5×10^5 cells/ 200 µl/well) with or without HMPH at different concentrations for 24 h in humidified 5% CO_2, with or without 100 ng/ml LPS. TNF-α in supernatant was estimated by sandwich ELISA following manufacturer's instructions (eBioscience, Cat# 88-7346-88).

2.2.3. In vivo screening assays

2.2.3.1. Animals. All experiments employed Sprague-Dawley rats of either sex, 180-230 g, obtained from Central Animal Research Facility, Manipal University, housed in plastic cages with 12 h light/dark cycle at 26 ± 1 °C and 50 ± 5 % humidity and fed with standard food pellet and water *ad libitum*. The experimental protocol was approved by the Institutional Animal Ethical Committee (Ref No. IAEC/KMC/55/2013).

2.2.3.2. Acute toxicity test. Acute toxicity was evaluated as per OECD 420 guidelines. Rats were administered a maximum dose of 2000 mg/kg orally and were observed individually every 30 min up to 4 h and subsequently every 6-8 h for 14 days for signs of toxicity.

2.2.3.3. Drug treatment regimen. HMPH at 12.5, 25 and 50 mg/kg, was administered to rats (n=6, per group) by intraperitoneal route once daily in 0.25 % w/v CMC as suspension (Table 2). Diclofenac sodium (10 mg/kg) was used as reference standard.

Table 2

Treatment regimen of HMPH in individual studies.

No.	Experiments	Days of Treatment	Dose Schedule	Dose of HMPH
1.	Carrageenan-induced acute paw edema	5 days	Prophylactic	25 and 50 mg/kg
2.	Carrageenan-induced acute air-pouch	5 days	Prophylactic	12.5, 25 and 50 mg/kg
3.	LPS-induced acute lung inflammation	5 days	Prophylactic	25 and 50 mg/kg
4.	CFA-induced arthritis	14 days	Treatment	12.5, 25 and 50 mg/kg

2.2.3.4. Carrageenan-induced paw-edema. HMPH was administered to SD-rats for five days before carrageenan challenge. On fifth day, 15 min after HMPH dosing, 0.1 ml of freshly prepared carrageenan (1 % w/v in normal saline) was injected to left hind paw (sub-plantar). Paw volumes were measured at 0 (basal reading), 1, 2, 3 and 5^{th} hour after carrageenan challenge using digital plethysmometer (37140; Ugo Basile S.R.L., Italy). Paw volumes of test and control rats, at each time points, were tested for statistically significant differences [20].

2.2.3.5. Carrageenan-induced air-pouch model in rats. Air-pouch inflammation was developed as per established protocol [21] with minor modifications. On day 1, air-pouch was developed by injecting 20 ml of sterile-air subcutaneously, through 0.22 mm syringe filter unit (Millipore, USA) to the shaved dorsal part (below neck region). To maintain the air-pouch, 10 ml of air was injected into the same sack on day 3 and 5. On day 5, after 30 min of HMPH administration (Table 2), 2 ml of 1% w/v carrageenan was injected to each air-pouch to trigger inflammation in all groups except naive controls, which received normal saline. Blood was collected from retro orbital plexus after 6 h of carrageen-induction. Blood, air-pouch-lavage and spleen (after sacrifice) collected, to test the inflammatory markers (section 2.2.3.8 to 2.2.3.11). TNF-α in lavage was estimated by ELISA according to manufacturer's instructions (Cat# RTA00, Quantikine ELISA kit, R&D Systems).

2.2.3.6. LPS-induced lung inflammation model. A standard method was followed with some modifications [22]. Thirty min after HMPH/diclofenac treatment (Table 2), rats were challenged with 50 µg/ml/kg of LPS in normal saline by intra-tracheal route. Rats were euthanized after 4h of LPS instillation and BAL collected for differential cell count estimation (sections 2.2.3.9).

2.2.3.7. CFA-induced arthritis model. CFA was freshly prepared with *Mycobacterium butyricum* (Product# 264010, DIFCO) as suspension in paraffin oil (Merck). On day 1, rats received intraplantar injections (left hind paws) of 0.1 ml of 5 mg/ml of CFA. Naive controls received 0.1 ml paraffin oil. Rats were divided into different treatment groups based on left-hind paw-volume on day 7. Treatment with HMPH and diclofenac (Table 2) continued from day 14 to 21. B.wt., clinical scoring, ipsilateral and contralateral paw volumes were measured on day 1, 7, 14 and 21. Percentage change in B.wt. was calculated [formula: ((day 'x' B.wt. – day 1 B.wt.)/day 1 B.wt.) × 100]. The severity of arthritis was evaluated by [a] macroscopically by clinical scoring [b] radiographic changes and [c] hematological parameters using Veterinary Blood Cell Counter (PCE-210VET, Erma Inc., Tokyo, Japan). Rats were sacrificed on day 22 and the spleen, thymus, brain were isolated, blotted dry, weighed and tested for inflammatory markers (section 2.2.3.8, 2.2.3.10 and 11). Serum C-RP (Cat# MBS268328, MyBioSource, USA), RF (Cat# MBS260028, MyBioSource) and TNF-α (Cat# RTA00, Quantikine ELISA kit, R&D Systems) were estimated as per manufacturer instructions [21, 23, 24].

2.2.3.7.1. Clinical scoring and evaluation of arthritis development. From day 7 onwards arthritis was evaluated by macroscopic parameters such as ability to walk, redness of skin and swelling at ankle/wrist. Severity of arthritis was scored by grading each paw from 0 to 4 based on erythema, swelling and deformity of joints [25].

0 = No erythema or swelling

1 = Slight erythema or swelling of one of the toes or fingers

2 = Erythema and swelling of more than one toe or finger

3 = Erythema and swelling of the ankle or wrist

4 = Complete erythema and swelling of toes/fingers and ankle/wrist and inability to bend ankle/wrist. (Example – If all 4 legs are scored, highest possible arthritic index is 16).

2.2.3.7.2. Radiological and histopathological analysis. On day 21, rats were anesthetized and radiographs of the ipsilateral and contralateral paws were taken using x-ray (Model 2100, Kodak Co., Japan; 60 kV peak, 8 mA, exposure 0.08 sec; focus distance = 40-50 inches) [21].

Rats were sacrificed (day 22) by cervical dislocation, hind paw ankles amputated, fixed in 10 % neutral-buffered formalin, decalcified in 10 % formic acid, dehydrated, processed and embedded in paraffin. Five micron sections were stained (hematoxylin and eosin) and evaluated in a blinded manner for histopathological assessment of cellular infiltration, synovial hyperplasia, pannus formation, bone and cartilage erosion of ankle joints [23].

2.2.3.8. Blood collection and processing. In carrageenan-induced air-pouch model, blood was withdrawn from retro-orbital plexus at 6 h after carrageenan into tubes with 10 % K_2-EDTA to prevent coagulation. On day 21, in CFA-induced arthritis model, blood was collected in centrifuge tubes with and without K_2-EDTA. Plasma was separated by centrifugation (8000 rpm; 10 min, at 4 °C) using cooling micro-centrifuge (MIKRO 22R, Andreas Hettich GmbH & Co.KG, Germany) and serum was separated (centrifuge, 5000 rpm for 12 min). Plasma/serum aliquots were stored in -80 °C before estimation of inflammatory markers. Whole blood was processed for hematological analysis before plasma/serum separation using the Veterinary Blood Cell Counter (PCE-210VET, Erma Inc., Japan). Percentage Cell count changes were calculated.

2.2.3.9. Collection and processing of lavages. Rats were sacrificed after 6 h of carrageenan challenge, the air-pouch washed 3 times with 5 ml of chilled sterile saline, lavage collected with gentle massage, volume measured and total leucocyte count measured by a Veterinary Blood Cell Counter. In LPS-induced lung inflammation model, rats were euthanized (by ketamine and xylaxine injection) and lung-lavage was collected (by washing 3 times with 5 ml ice-cold HBSS) and centrifuged (4500 rpm/10 min, 4 °C). The pellet obtained was re-suspended in 2 ml of HBSS, and total leukocyte count estimated. Aliquots of lavages were stored at -80 °C for further analysis. Percentage change in both air-pouch and lung lavage was calculated [formula: (absolute cell count of each rat/average cell count of carrageenan control or LPS control) × 100].

2.2.3.10. Splenomegaly and thymus atrophy. Splenomegaly was assessed by the ratio of spleen weight to B.wt. Inhibition of thymus atrophy was determined from changes in the ratio of thymus weight/ brain weight [23].

2.2.3.11. MPO and nitrite activity. MPO in lavages and serum was determined by the method reported previously with minor changes [26]. Briefly, 125 µl of *O*-dianisidine HCl (ODA, 1.67 mg/10 ml in 50 mM phosphate buffer, pH 6) containing 0.5 % v/v hydrogen peroxide was added to 25 µl of lavage/serum, incubated for 30 min in dark at room temperature, 25 µl of 4M H_2SO_4 was added to stop reaction and absorbance was recorded (λ= 490 nm) using microplate reader. Nitrite levels were estimated in both lavage-fluid and in serum by using Griess Reagent.

2.2.3.12. Statistical Analysis. Statistical analysis was performed by using GraphPad Prism 6.01. Data are represented as mean ± SEM and evaluated by one-way and two-way ANOVA followed by Dunnett's multiple comparison test ($p<0.05$ = statistically significant).

3. Results and discussion

3.1. Cytoprotective effect of HMPH on RAW 264.7 murine macrophages

HMPH was non-toxic to RAW 264.7 macrophages with IC_{50} exceeding 1000 µM. Therefore 0.5 to 500 µM was considered safe for *in vitro* experiments.

3.2. LPS-induced in vitro inflammation in RAW 264.7 cell lines

HMPH dose-dependently decreased LPS-induced extracellular-nitrite and intracellular-ROS in RAW 264.7 cells (Table 3), indicating a protective role by attenuating the LPS-TLR4 inflammatory signaling cascade at low concentrations [27]. ROS and nitrite release were comparable to that of DPI and L-NAME, respectively.

Table 3

IC_{50} value of HMPH for ROS inhibition and nitrite inhibition assay.

Sl. No.	Compounds	*In vitro* ROS inhibition	*In vitro* Nitrite inhibition
1.	DPI (5µM)	90 ± 3%	-
2.	L-NAME (100µM)	-	35 ± 2%
3.	HMPH	IC_{50} 3.5 ± 0.7 µM	IC_{50} of 2.4 ± 0.4 µM

3.3. Free radical scavenging property of HMPH

HMPH scavenged DPPH and ABTS radicals in a dose dependent manner (data not shown), with IC_{50} comparable to curcumin. HMPH scavenged DPPH radicals more powerfully than curcumin (Table 4). The electron transfer ability of HMPH in the scavenging process of ABTS radical anion was less than curcumin (IC_{50} of HMPH= 298 ± 40 Vs curcumin= 48 ± 4 µM, Table 4). Antioxidant property of HMPH may play a role in anti-inflammatory activity [14].

3.4. Inhibition of lipid peroxidation by HMPH

HMPH inhibited LPO in rat brain with comparable efficacy to α-tocopherol (Table 4).

LPO significantly contributes to inflammation and cancer. Apart from anti-oxidant property, HMPH also inhibits iron-catalysed lipid peroxidation, which is implied in inflammation [17].

Table 4

IC_{50} values of HMPH for DPPH/ABTS free radical scavenging assay and lipid peroxidation inhibition assay.

Sl. No.	Compounds	*DPPH free radical scavenging Assay*	*ABTS free radical scavenging Assay*	*Lipid peroxidation Assay*
1.	α-Tocopherol	-	-	58 ± 8 µM
2.	Curcumin	44 ± 5 µM	48 ± 4 µM	-
3.	HMPH	29 ± 6 µM	298 ± 40 µM	135 ± 9 µM

Data presented as mean ± SEM (n=3).

3.5. The action of HMPH on COX-2 enzyme

Antioxidant property of HMPH raised questions about its role in COX inhibition. COX-1 plays a homoeostatic role while COX-2 is inducible in acute inflammation, while HMPH, up to 25 µM did not inhibit COX-2. Even at 250 µM, COX-2 inhibition was just 20 %.

3.6. Prevention of TNF-α release in mouse peritoneal macrophages and in human PBMCs

The insignificant COX enzyme inhibition and profound decrease in LPS-induced nitrite and ROS in murine macrophages by HMPH together suggests a probable mode of action via LPS-TLR and TNF pathway. Therefore, HMPH was tested for inhibiting TNF-α in mouse peritoneal-macrophages and in human PBMCs.

Macrophages release many chemokines, which play important roles in homeostasis and inflammation. Among chemotactic cytokines, TNF-α plays an important immune-regulatory role [28, 29]. The mouse peritoneal-macrophage is a very important player in infections, inflammatory morphology and pathology besides the maintenance of immune response [30-33].

PBMCs (a primary cell line) is the chief component in the immune system that fights infections. PBMCs include lymphocytes, monocytes and dendritic cells. The lymphocyte population consists of T-cells (CD4 and $CD8^+$), B-cells and NK-cells, which play a major role in immune defence. During LPS-challenge, monocytes and macrophages are the first to get activated, which in turn produces IL-1β, TNF-α and IL-6 [34, 35].

LPS triggers the innate immune system by binding to LBP (LPS-binding protein, an acute-phase protein) and catalysing the transfer of LPS to membrane-bound CD14 (mCD14, a 55-kDa glycoprotein) expressed on the surface of monocytes. LPS is released into the lipid bilayer from CD14. LBP disintegrates the LPS aggregates into smaller units during intercalation into phospholipid cell matrix. Subsequently, the free-LPS binds to receptors such as chemokine receptor-4 [36]. This inflammatory trigger activates the TLR signaling, followed by activation of NF-κB signal-transduction pathways [36, 37]. HMPH dose dependently (50 to 200 µM) attenuated LPS-induced TNF-α release significantly in mouse peritoneal macrophages (Fig. 2a) and in human PBMCs (Fig. 2b). HMPH decreased TNF-α release probably by interfering with TLR/NF-κB cascade in both mouse peritoneal macrophages and in human PBMCs, thereby stabilizing immune system.

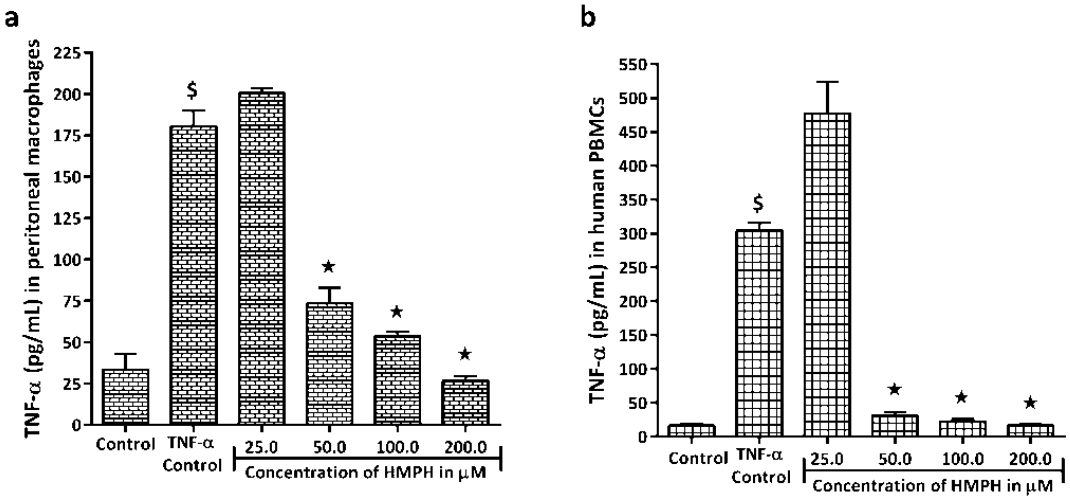

Fig. 2. Effect of HMPH (25 to 200 mg/kg) on LPS-induced TNF-α in (a) mouse peritoneal macrophages and (b) human PBMCs. Data presented as mean ± SEM (n=3). $p<0.05 vs naïve control and ★p<0.05 vs TNF-α control (one-way ANOVA followed by Dunnett's multiple comparisons test).

3.7. The safety profile of HMPH in Rats

HMPH neither produced any death nor any visible symptoms of toxicity in rats up to 72 h at 2000 mg/kg/oral and 400 mg/kg/intraperitoneal dose. Results suggest that HMPH has a large window of safety.

3.8. Inhibition of acute paw inflammation by HMPH

After ascertaining the *in vitro* anti-inflammatory activity mediated via TNF-α pathway, HMPH was tested for *in vivo* activity with positive results in carrageenan-induced paw edema. (Fig. 3). HMPH, at 25 and 50 mg/kg doses, reduced the paw-volume at all time-points and was significant at 5^{th} h (Fig. 3). The local inflammation was significantly reduced by diclofenac at 1, 2, 3 and 5 h. However, inhibition of inflammation began to decline from the 5^{th} h, probably because of systemic clearance of diclofenac (diclofenac plasma t_{max} varies from 1 to 4.5 h after single dose and half-life is 1.8 h) [38]. Unlike diclofenac, the activity in HMPH was significant particularly after the third hour, possibly indicating a delayed onset and prolonged duration of action, thereby predicting a role in chronic therapy.

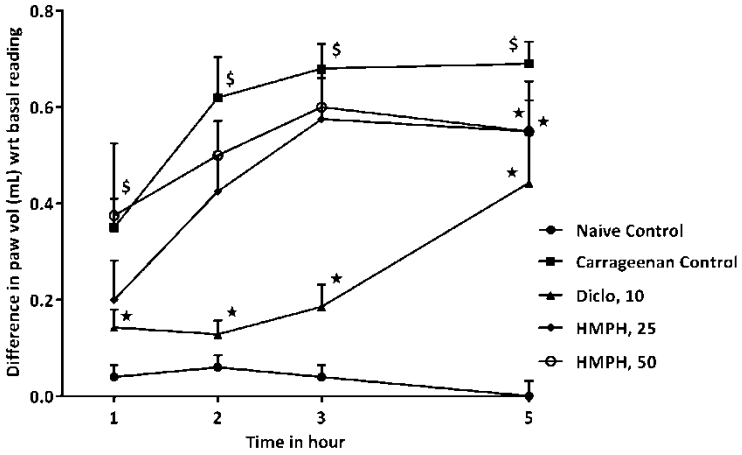

Fig. 3. Attenuation of carrageenan-induced acute paw inflammation by HMPH (25 and 50mg/kg) and diclofenac (10 mg/kg). Figure depicts changes in the paw volume (ml) at various time points. Data presented as mean ± SEM (n=6). $p<0.001 vs naïve control. ★p <0.05 vs carrageenan control (Two-way ANOVA followed by Dunnett's multiple comparisons test).

3.9. Attenuation of inflammatory markers in air-pouch model

This model of acute inflammation represents a primary immunological response to invading pathogens and help understand the local and systemic effects of compounds on

immune cells and inflammatory mediators [20]. The following sections (3.9.1. to 3.9.3.) discuss the effects of HMPH action on MPO, nitrite, TNF-α and differential cell count in air-pouch lavage.

3.9.1. Reduction of splenomegaly in air-pouch model by HMPH

HMPH, at all tested doses mildly attenuated splenomegaly, though not significantly ($p>0.05$, data not shown). Splenomegaly in carrageenan-control indicates immunological response [23], which was annulled significantly by diclofenac.

3.9.2. Reversal of elevated MPO and nitrite by HMPH in air-pouch model

Elevated nitrite and MPO in air-pouch lavage and plasma indicate an immunological response. MPO helps neutralize invading pathogens and is a marker of leukocyte infiltration to the site of inflammation. HMPH dose-dependently decreased MPO in both plasma and air-pouch lavage (Fig. 4a and 4b) but more significantly in air-pouch lavage (Fig. 4b) which was comparable to diclofenac. MPO is normally present in the inactive form in circulating neutrophils. On reaching the site of inflammation, neutrophils undergo activation. It releases a low concentration of MPO which is available for maximum biological activity. During neutrophil transit, MPO may also accumulate in infected-plasma [26]; which we observed in our study (Fig. 4a).

The rise in nitrite levels in the lavage is through iNOS [39]. HMPH significantly reduced the elevated nitrite levels in the lavage (Fig. 4c), probably by iNOS inhibition.

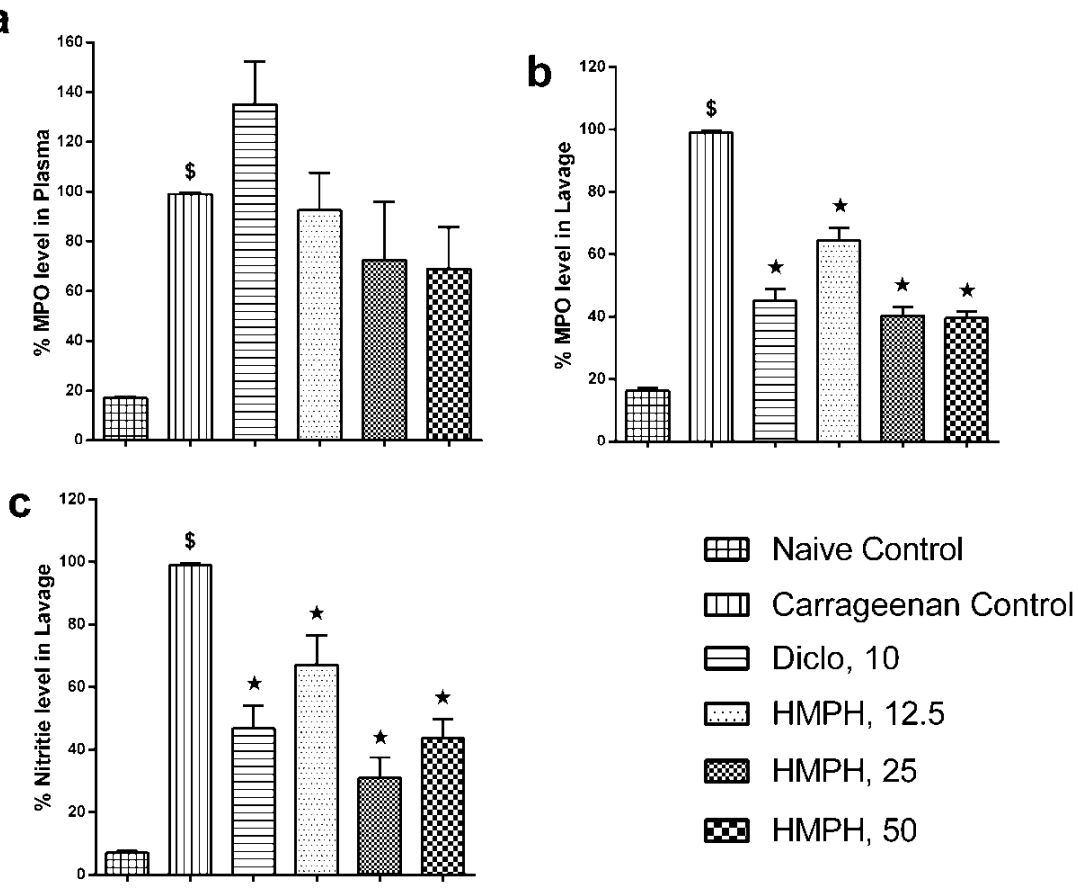

Fig. 4. Effect of HMPH (12.5 to 50 mg/kg) on MPO and nitrite in both (a) plasma and (b and c) in air-pouch lavage. Percentage change was calculated with respect to carrageenan-control. Data presented as mean ± SEM (n=5). $p<0.05 vs naïve control and ★p<0.05 vs carrageenan control (one-way ANOVA followed by Dunnett's multiple comparisons test).

3.9.3. Inhibition of cellular infiltration in air-pouch lavage by HMPH

Air-pouch is self-possessed of a lining of cells that consists primarily of macrophages and fibroblasts, which produces an inflammatory granulomatous reaction characterized by marked production of inflammatory mediators in lavage [40]. HMPH significantly and dose dependently decreased the total WBC count (Fig. 5a) and differential counts (lymphocytes and monocytes) in air-pouch lavage (Fig. 5b and 5c). The absolute cell counts in naïve-control and carrageenan-control were found to be 1.3 ± 0.24 and 27.3 ± 2.72 × 10^3/µl in total WBC, 0.93 ± 0.17 and 21 ± 1.68 × 10^3/µl in total lymphocytes and 0.07 ± 0.0 and 1.9 ± 0.25 × 10^3/µl in monocytes respectively. HMPH (25 and 50 mg/kg) significantly decreased TNF-α in air-pouch lavage (Fig. 5d), whereas diclofenac failed [20]. TNF-α may be the primary cytokine which is synthesized by activated macrophages and neutrophils during cell injury.

TNF-α, in turn, activates the release of other pro-inflammatory mediators which are also responsible for autoimmune disorders [41]. Anti-inflammatory action of HMPH is probably the result of attenuating TNF-α in air-pouch lavage (Fig. 5d). Probably, HMPH also modulates the immune system by suppressing not only the total WBC count, but also lymphocytes and monocytes in the lavage (Fig. 5a, 5b and 5c).

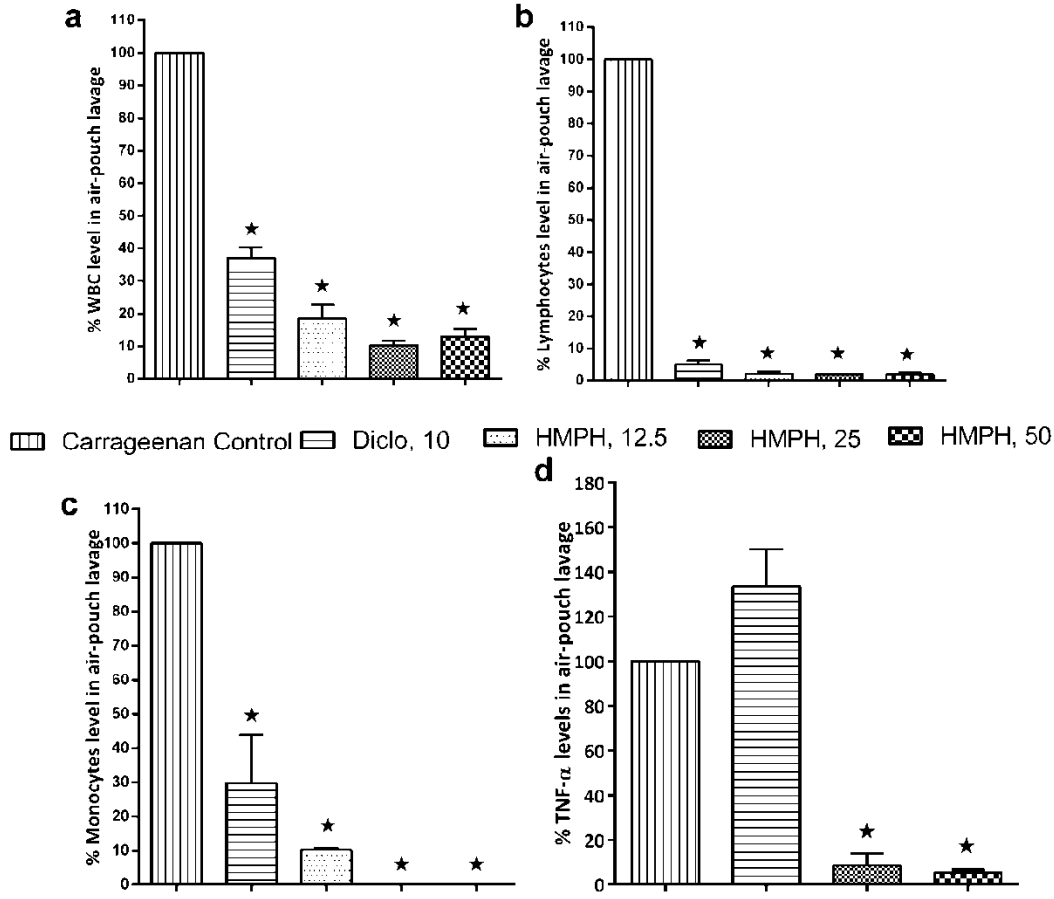

Fig. 5. Influence of HMPH (12.5 to 50 mg/kg) and diclofenac (10 mg/kg) on (a) total WBC count (b) lymphocytes, (c) monocytes and (d) TNF-α in air-pouch lavage with respect to carrageenan control. Percentage change was calculated by considering respective carrageenan-control as 100 %. Data presented as mean ± SEM (n=5). ★$p<0.05$ vs carrageenan control (one-way ANOVA followed by Dunnett's multiple comparisons test).

3.10. The effect of HMPH on cellular-infiltration in bronchoalveolar lavage

LPS induces cellular responses that develop symptoms of chronic lung function-injury in rats, which is similar to those caused by organic dust exposure in humans. Intra-tracheal LPS-induction elevated the cellular response reflecting proportionately in BAL fluid [42].

LPS-treatment increased total WBC, lymphocytes and granulocytes count in the BAL by 20-25 % compared to naïve control. The absolute cell count in naïve-control and LPS-control were 0.6 ± 0.1 and 2.1 ± 0.2 × 10^3/µl for WBC, 0.35 ± 0.1 and 1.2 ± 0.1 × 10^3/µl for total lymphocytes and 0.15 ± 0.0 and 1.0 ± 0.1 × 10^3/µl for granulocytes respectively. HMPH produced a dose dependent attenuation of lung inflammation by reducing total WBC and differential cell counts in BAL fluid (Fig. 6). Maximum activity was observed at HMPH 50 mg/kg (Fig. 6a and 6c), indicating the inhibition of chemotaxis during inflammation.

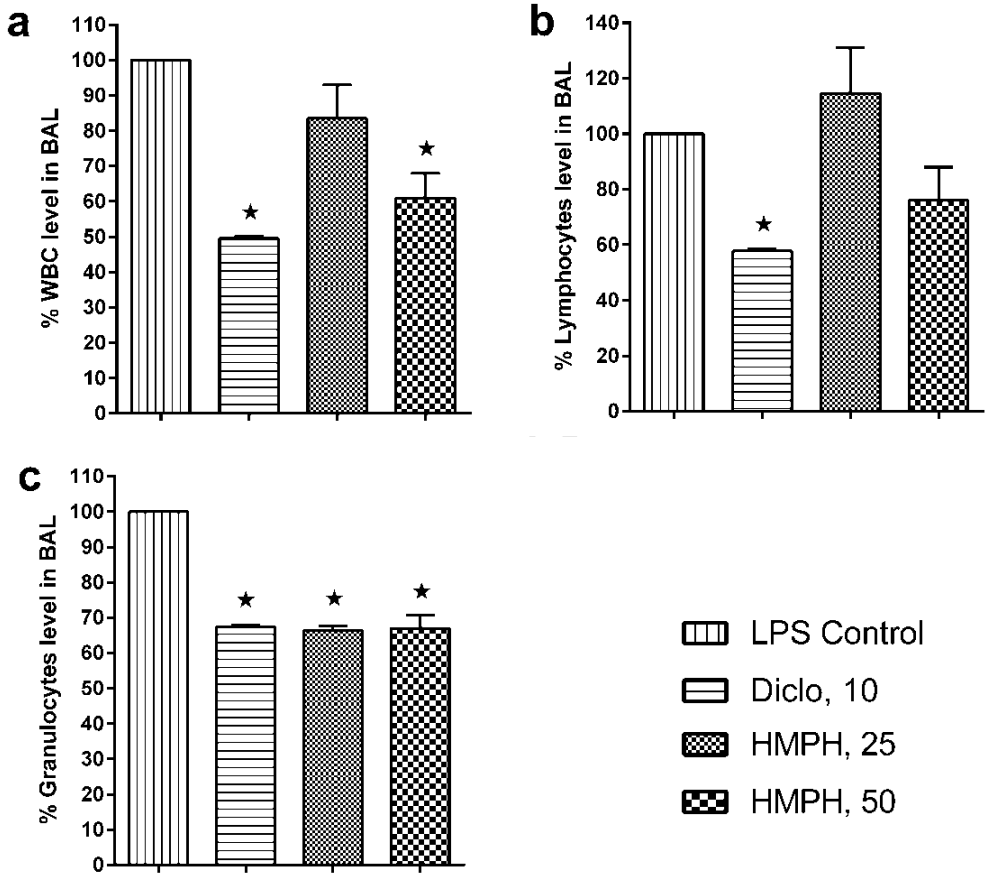

Fig. 6. Effect of HMPH (25 and 50 mg/kg) and diclofenac (10 mg/kg) on (a) total WBC count, (b) lymphocytes and (c) granulocytes in BAL. Percentage change was calculated by considering respective LPS-control as 100 %. Data presented as mean ± SEM (n=5). ★p<0.05 vs LPS control (one-way ANOVA followed by Dunnett's multiple comparisons test).

3.11. HMPH attenuated the severity of arthritis

HMPH, having demonstrated activity in acute and sub-acute models of inflammation, by attenuating leukocyte-infiltration and limiting TNF-α, we thought it appropriate to consider the action of HMPH in chronic inflammation related to immune mediated

phenomena. AIA in rats was chosen because it has components of both local and systemic inflammation [23]. AIA pathology resembles human arthritis involving cartilage destruction and bone resorption [43], which are easily noticeable in our study. HMPH attenuated acute and chronic inflammation and facilitated recovery as measured by decreasing paw inflammation, diminishing arthritic markers, increasing clinical scores and mitigating joint damage. The results are discussed in sections 3.11.1 to 3.11.4.

3.11.1. Effect of HMPH on body weight, clinical scoring and paw inflammation AIA model

HMPH reversed (after 6 days of treatment) basic symptoms of arthritis such as decrease in B.wt. and increase in clinical scorings (Fig. 7a and 7b). HMPH also reduced leukocyte count (Fig. 8), thymus weight (Fig. 9a) and attenuated splenomegaly.

In AIA model, development of paw-inflammation is biphasic, i.e., acute phase (day 1 to 8) and chronic phase (day 9 to 21). Contralateral paw inflammation develops during 2nd week after CFA injection (probably an immunological response) [44]. In our experiment, HMPH significantly decreased the increased paw volume in both ipsilateral (Fig. 7c) and contralateral paws (Fig. 7d) from day 14 onwards, indicating that HMPH is effective against both acute and chronic inflammation as well as immune-mediated inflammation.

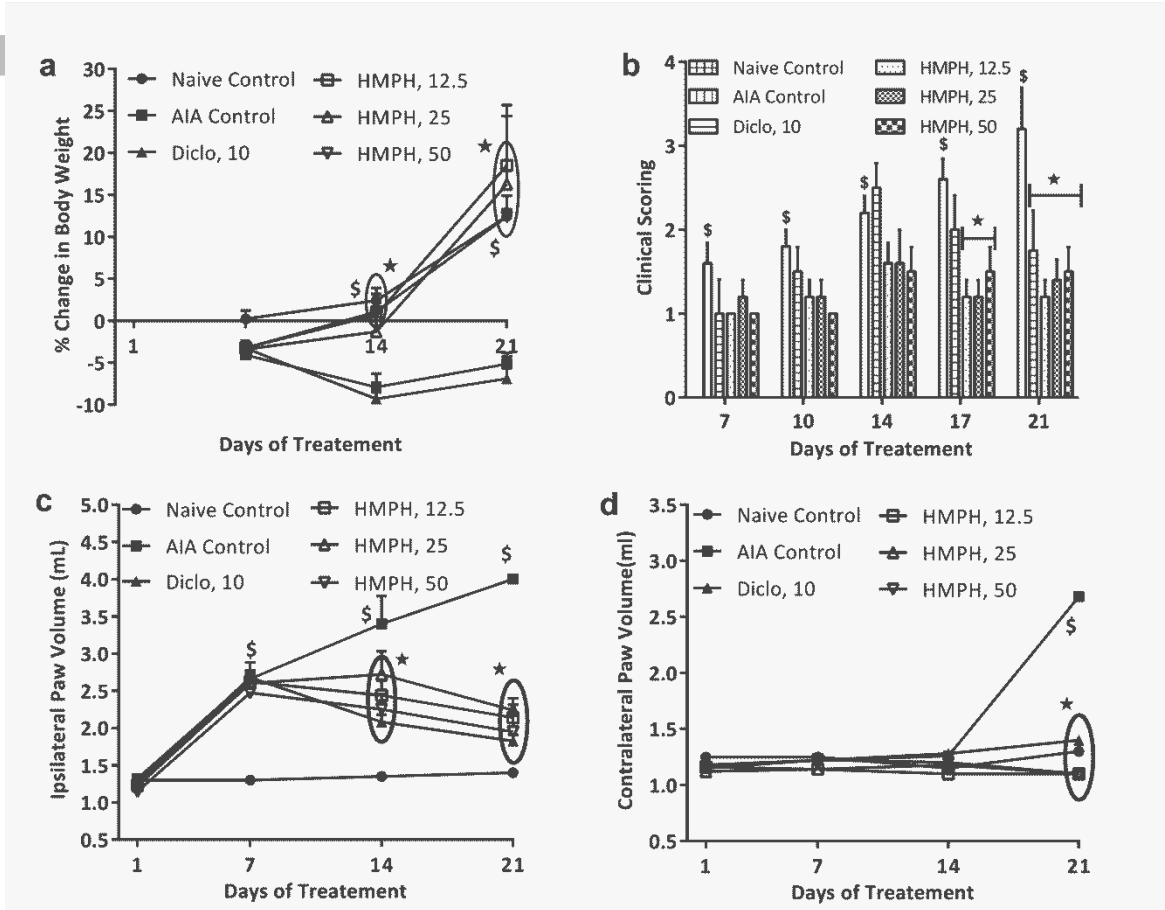

Fig. 7. Results of HMPH (12.5 to 50 mg/kg) and diclofenac (10 mg/kg) treatment on (a) % change in body weight on day 1, 7, 14 and 21, (b) clinical scoring (c) ipsilateral and (d) contralateral paw inflammation. All parameters have been compared with respective day AIA control. Data presented as mean ± SEM (n=6). $p<0.05 vs naïve control ★p<0.05 vs AIA control (two-way ANOVA followed by Dunnett's multiple comparison test).

3.11.2. Immunological support of HMPH in AIA rats

AIA is characterized by leukocytosis (lymphocytosis, monocytosis and granulocytosis), with extensive systemic neutrophilia [23]. HMPH (25 and 50 mg/kg) decreased the percentage WBC, lymphocytes, monocytes and granulocytes (Fig. 8) on day 21, suggesting an immuno-modulatory activity. HMPH 50 mg/kg profoundly decreased lymphocytes and monocytes (Fig 8b and 8c). However, diclofenac did not have any impact on leucocyte count. The absolute cell count in naïve-control and AIA-control were 7.0 ± 0.5 and 11.0 ± 1.3 × 10^3/µl for total WBCs, 5.0 ± 0.7 and 7.0 ± 0.8 × 10^3/µl for lymphocytes, 0.9 ± 0.1 and 1.7 ± 0.4 × 10^3/µl for monocytes and 0.4 ± 0.09 and 1.9 ± 0.5 × 10^3/µl for granulocytes respectively.

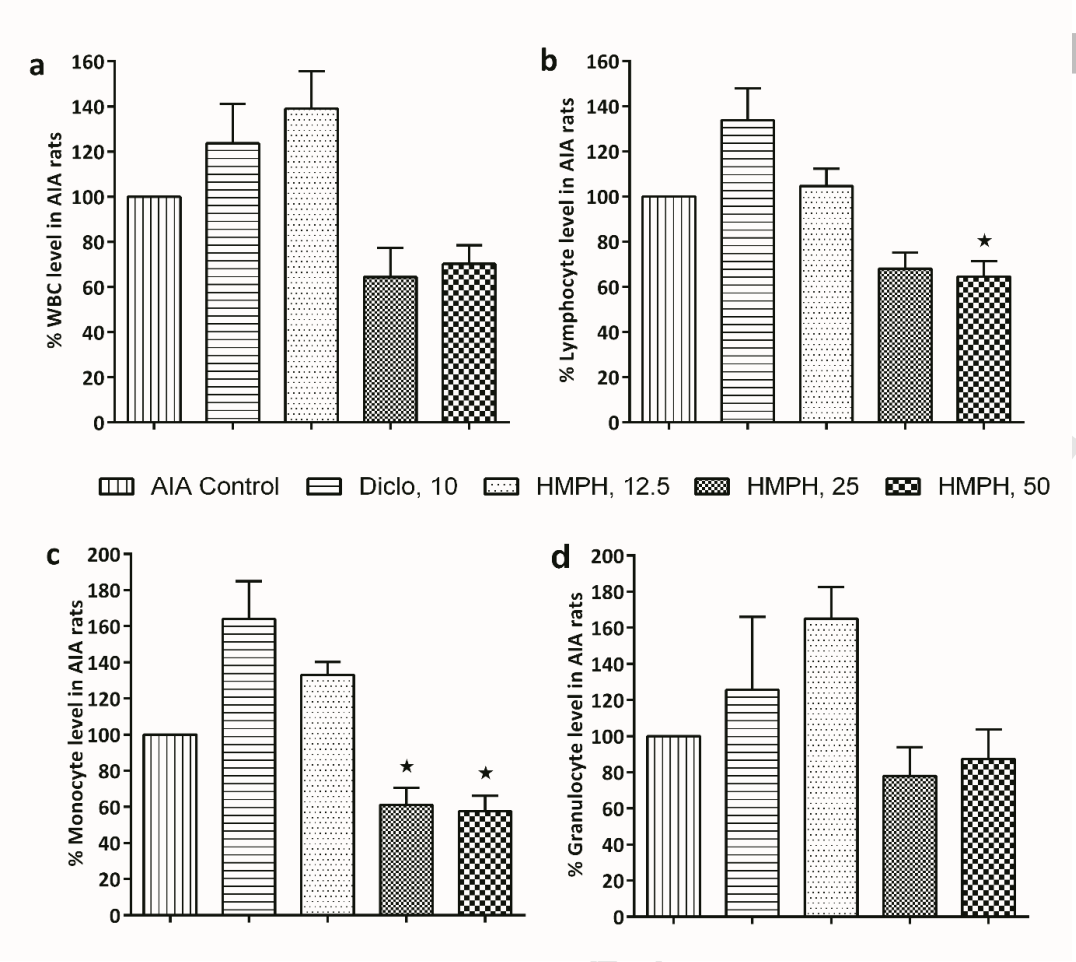

Fig. 8. Effect of HMPH (12.5 to 50 mg/kg) and diclofenac (10 mg/kg) on (a) WBC, (b) lymphocytes, (c) monocytes and (d) granulocytes on day 21 in blood. Percentage change was calculated by considering respective AIA-control as 100 %. Data presented as mean ± SEM (n=5).★$p<0.05$ vs AIA control (one-way ANOVA followed by Dunnett's multiple comparison test).

3.11.3. Effect of HMPH on serum C-RP, RF and TNF-α in AIA rats

HMPH (12.5 and 50 mg/kg) reduced the elevated serum C-RP, whereas diclofenac did not (Fig. 9b). C-RP is an acute-phase protein produced by hepatocytes that rises during tissue trauma, bacterial infections and inflammatory reactions like rheumatoid arthritis in cartilage and bone [21, 23].

HMPH (50 mg/kg) and diclofenac attenuated RF significantly (Fig. 9c). In the present study there was more than a three-fold increase in RF in AIA-control, implying a greater-probability of articular destruction with suspected autoimmune disease [21].

TNF-α levels being lower in the serum than in the inflammatory tissues, we were not surprised to find that TNF-α was below detectable limits (Fig. 9d) [20]. We observed an

increase in TNF-α in HMPH and diclofenac treated arthritic animals. However, the similar nature of HMPH and diclofenac in raising TNF-α suggests that they share some mechanistic elements [24].

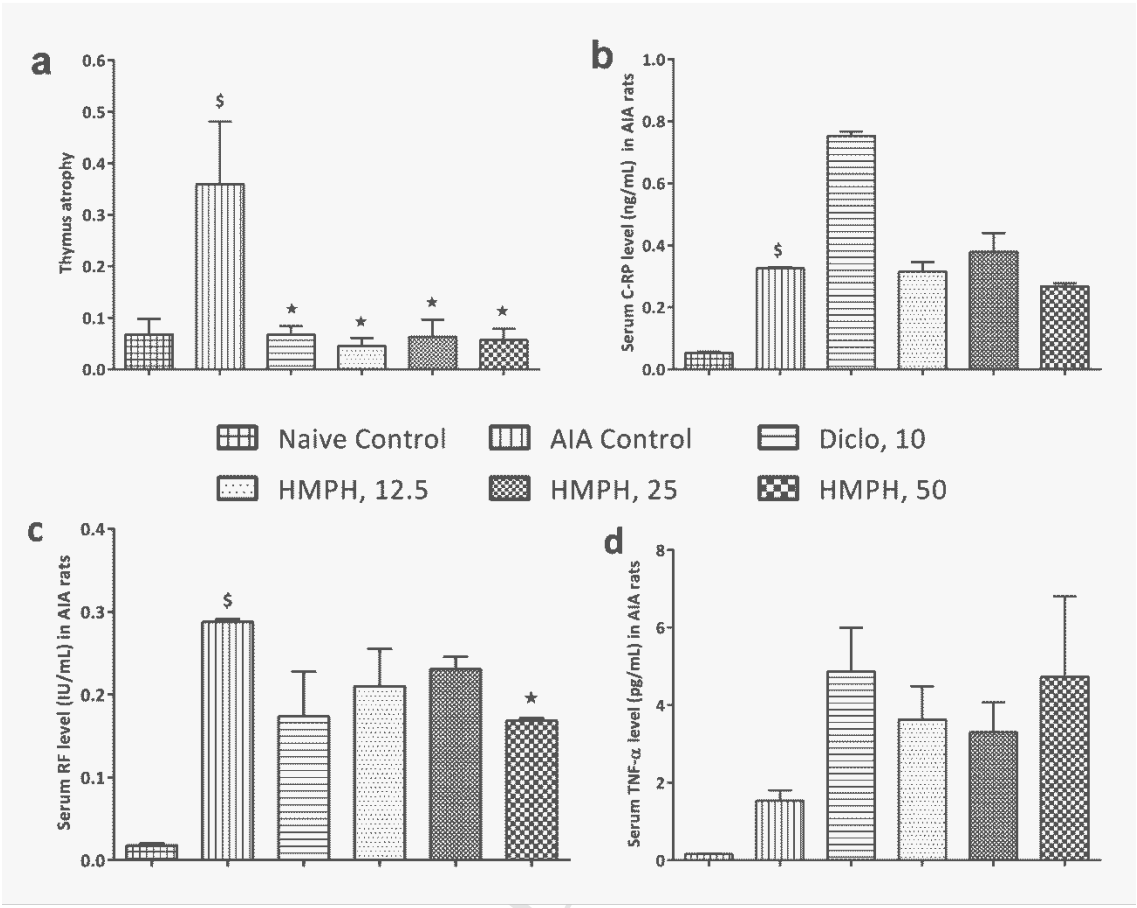

Fig. 9. Effect of HMPH (12.5 to 50 mg/kg) and diclofenac (10 mg/kg) on (a) thymus atrophy ratio, (b) serum C-RP, (c) serum RF and (d) serum TNF-α. Data presented as mean ± SEM (n=5). $p<0.05 vs naïve control, ★p<0.05 vs AIA control (one-way ANOVA followed by Dunnett's multiple comparison test).

3.11.4. HMPH improved radiographic and histopathological status in AIA model

Both HMPH (50 mg/kg) and diclofenac diminished soft tissue swelling, cystic enlargement of bone, extensive erosion and bone destruction as per radiographic impression and histopathological study. The differences were substantial when compared to AIA-control. The efficacy of HMPH is comparable to diclofenac.

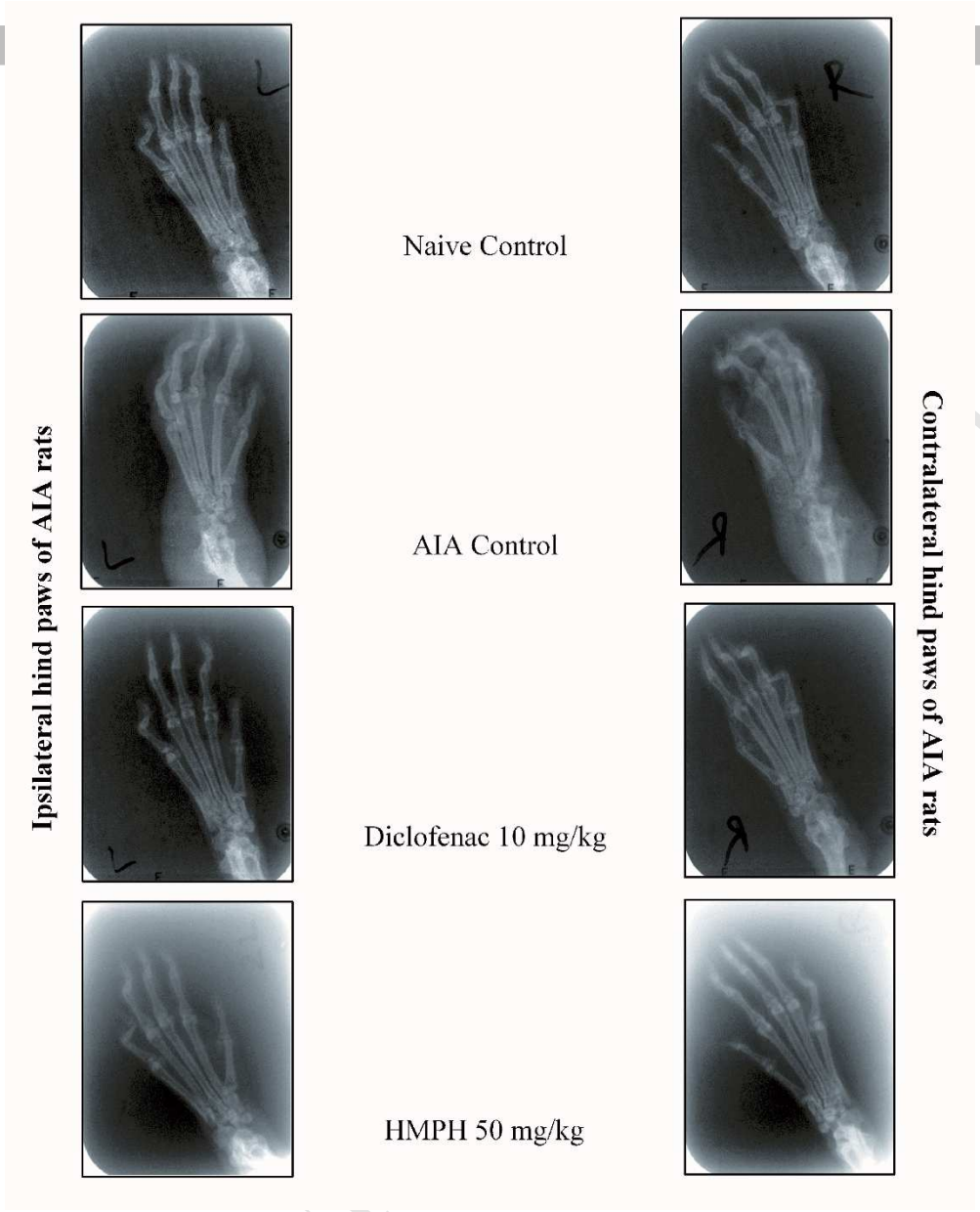

Fig. 10. Effect of HMPH on radiographic impressions in AIA rats (representative from each group of treatments). On day 21, Ipsilateral and contralateral hind paw images were captured under anaesthesia. The intensity of swelling and bone distortion was analysed with respect to naïve control.

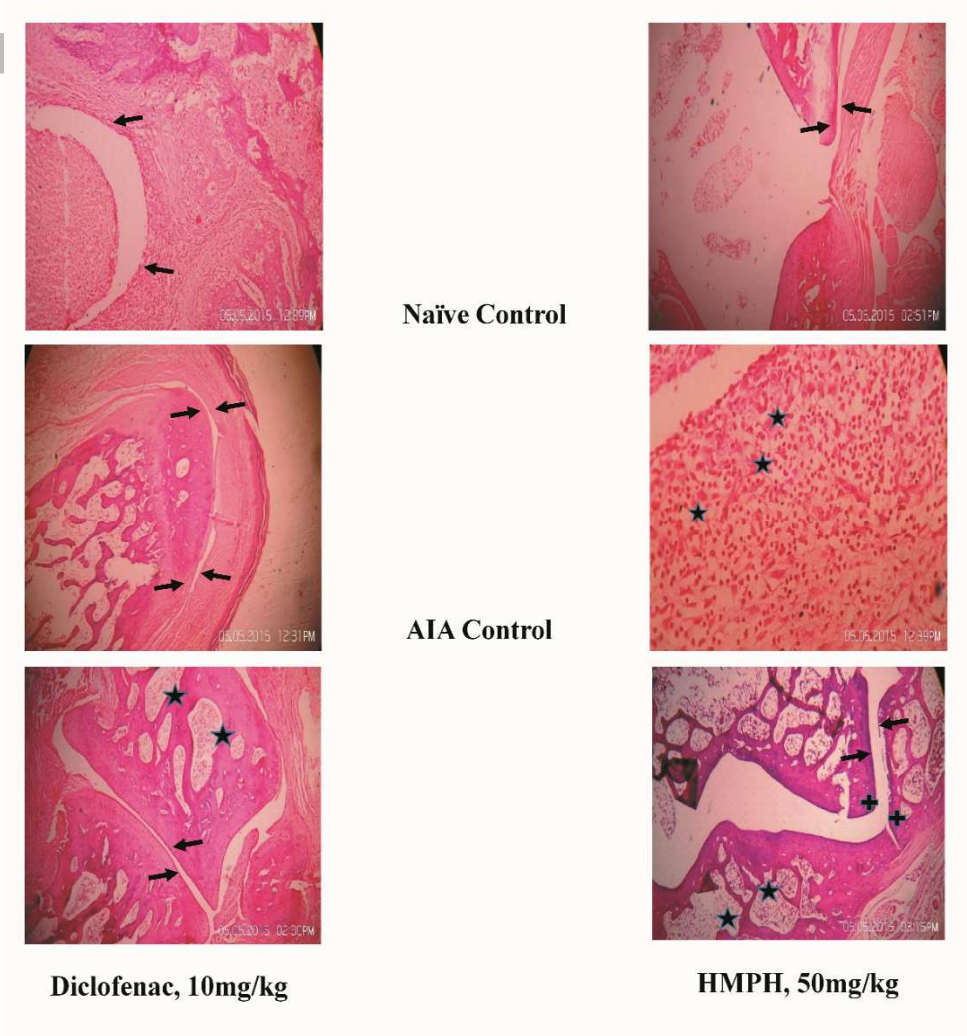

Fig. 11. Effect of HMPH on hind paw joint histopathology (synovial joint) in AIA rats (representative from each group of treatments). In naïve control group, the black arrows indicate normal surfaces of synovial joint with normal joint space and synovium. In AIA control group, black arrow indicates destructed synovial joint with reduced joint space (one surface pushing towards the other forming pannus), ★ indicates the presence of dense inflammatory cells (lymphocytes and plasma cells). In diclofenac 10mg/kg treatment, the black arrows indicate normal surfaces of synovial joint and ★ indicates presence of mild inflammation. In HMPH 50 mg/kg treatment, the black arrow indicates normal surface of synovial joint and ★ depicts mild inflammation and mild joint destruction (+ sign).

4. Conclusion

HMPH was synthesised by an easy one-step synthetic method under mild laboratory conditions with high yields. HMPH with low toxicity was effective against both acute and chronic inflammation in *in vitro* and *in vivo* models. The immune-modulatory effect of HMPH was significant in blood and body fluids at the site of inflammation. HMPH was similar to diclofenac in efficacy and more effective in chronic inflammatory conditions. HMPH reduced joint inflammation and bone erosion with an efficacy that was comparable to diclofenac. However, HMPH does not operate via COX unlike diclofenac. Molecular

mechanistic study revealed that HMPH might be operating more through an immuno-modulatory mechanism, via TLR/TNF-α pathway. To sum up, easy inexpensive synthetic route with high yield, favorable chemical characteristics, low toxicity and high efficacy via non-COX mediated pathway suggests that HMPH could be studied further as a potential lead for chronic inflammatory condition.

Conflict of Interest

The authors confirm that we do not have any conflict of financial interest.

Acknowledgements

This work is funded by the Department of Biotechnology (DBT), India (BT-Indo-Qld/01/06/2010). We are grateful to the Department of Pharmacology and Pharmacy Practice of Manipal College of Pharmaceutical Sciences and Manipal University, Karnataka, Manipal-576104 for providing the conveniences to carry out the research work. The authors are thankful to NMR Research Centre, IISc, Bangalore and NFDD center, Department of Chemistry, Saurashtra University, Rajkot, India for providing ^{1}H NMR and ESI-MS spectra, respectively.

References

[1] V. Fuster, J.M. Sweeny, Aspirin A Historical and Contemporary Therapeutic Overview, Circulation, 123 (2011) 768-778.

[2] C. Sostres, C.J. Gargallo, M.T. Arroyo, A. Lanas, Adverse effects of non-steroidal anti-inflammatory drugs (NSAIDs, aspirin and coxibs) on upper gastrointestinal tract, Best Pract Res Clin Gastroenterol, 24 (2010) 121-132.

[3] C.P. Cannon, P.J. Cannon, COX-2 inhibitors and cardiovascular risk, Science, 336 (2012) 1386-1387.

[4] R.G. Kurumbail, A.M. Stevens, J.K. Gierse, J.J. McDonald, R.A. Stegeman, J.Y. Pak, D. Gildehaus, J.M. Miyashiro, T.D. Penning, K. Seibert, Structural basis for selective inhibition of cyclooxygenase-2 by anti-inflammatory agents, Nature, 384 (1996) 644-648.

[5] C.A. Dinarello, Proinflammatory cytokines, Chest Journal, 118 (2000) 503-508.

[6] J. Bradley, TNF-mediated inflammatory disease, J Pathol, 214 (2008) 149-160.

[7] R.K. Singh, R. Tandon, S.G. Dastidar, A. Ray, A review on leukotrienes and their receptors with reference to asthma, J Asthma, 50 (2013) 922-931.

[8] M. Mertens, J.A. Singh, Anakinra for rheumatoid arthritis: a systematic review, J Rheumatol, 36 (2009) 1118-1125.

[9] P. Sarzi-Puttini, F. Atzeni, Y. Shoenfeld, G. Ferraccioli, TNF-alpha, rheumatoid arthritis, and heart failure: a rheumatological dilemma, Autoimmun Rev, 4 (2005) 153-161.

[10] M. Si, Y. Yan, L. Tang, H. Wu, B. Yang, Q. He, H. Wu, A novel indole derivative compound GY3 improves glucose and lipid metabolism via activation of AMP-activated protein kinase pathway, Eur J Pharmacol, 698 (2013) 480-488.

[11] J. Zong, W. Deng, H. Zhou, Z. Bian, J. Dai, Y. Yuan, J. Zhang, R. Zhang, Y. Zhang, Q. Wu, 3, 3′-Diindolylmethane protects against cardiac hypertrophy via 5′-adenosine monophosphate-activated protein kinase-alpha2, PloS one, 8 (2013) e53427.

[12] S. Ali, N. Ali, B. Ahmad Dar, V. Pradhan, M. Farooqui, Chemistry and biology of indoles and indazoles: a mini-review, Mini Rev Med Chem, 13 (2013) 1792-1800.

[13] M.R. Kandadi, P.K. Rajanna, M.K. Unnikrishnan, S.P. Boddu, Y. Hua, J. Li, M. Du, J. Ren, N. Sreejayan, 2-(3, 4-Dihydro-2H-pyrrolium-1-yl)-3oxoindan-1-olate (DHPO), a novel, synthetic small molecule that alleviates insulin resistance and lipid abnormalities, Biochem Pharmacol, 79 (2010) 623-631.

[14] K. Prabhakar, V. Veerapur, P. Bansal, K.P. Vipan, K. Reddy, A. Barik, B.K.D. Reddy, P. Reddanna, K. Priyadarsini, M. Unnikrishnan, Identification and evaluation of antioxidant, analgesic/anti-inflammatory activity of the most active ninhydrin–phenol adducts synthesized, Bioorg Med Chem, 14 (2006) 7113-7120.

[15] G. Mathew, A. Jacob, E. Durgashivaprasad, N.D. Reddy, M.K. Unnikrishnan, 6b,11b-Dihydroxy-6b,11b-dihydro-7H-indeno[1,2-b]naphtho[2,1-d]furan-7-one (DHFO), a small molecule targeting NF-kappaB, demonstrates therapeutic potential in immunopathogenic chronic inflammatory conditions, Int Immunopharmacol, 15 (2013) 182-189.

[16] P. Paul, P. Bansal, P.G. Nayak, S.T. Pannakal, K.I. Priyadarsini, M.K. Unnikrishnan, Polyphenolic fraction of Pilea microphylla (L.) protects Chinese hamster lung fibroblasts against gamma-radiation-induced cytotoxicity and genotoxicity, Environ Toxicol Pharmacol, 33 (2012) 107-119.

[17] Sreejayan, M.N.A. Rao, Curcumin inhibits iron-dependent lipid peroxidation, Int J Pharm, 100 (1993) 93-97.

[18] A. Ray, B.N. Dittel, Isolation of mouse peritoneal cavity cells, J Vis Exp, 28 (2010) pii: 1488.

[19] S.K. Panda, B. Ravindran, Isolation of Human PBMCs, Bio Protocol, 3 (2013) e323.

[20] J. Mudgal, V.S. Gowdra, G. Mathew, P.G. Nayak, N.D. Reddy, N. Namdeo, R.R. Kumar, C. Kantamaneni, M.R. Chamallamudi, G.K. Nampurath, Remedial effects of novel 2, 3-disubstituted thiazolidin-4-ones in chemical mediated inflammation, Chem Bio Interact, 210 (2014) 34-42.

[21] S. Talwar, K. Nandakumar, P.G. Nayak, P. Bansal, J. Mudgal, V. Mor, C.M. Rao, R. Lobo, Anti-inflammatory activity of Terminalia paniculata bark extract against acute and chronic inflammation in rats, J Ethnopharmacol, 134 (2011) 323-328.

[22] T. Ulich, S. Yin, K. Guo, J. Del Castillo, S. Eisenberg, R. Thompson, The intratracheal administration of endotoxin and cytokines. III. The interleukin-1 (IL-1) receptor antagonist inhibits endotoxin-and IL-1-induced acute inflammation, Am J Pathol, 138 (1991) 521-524.

[23] C. Balague, M. Pont, N. Prats, N. Godessart, Profiling of dihydroorotate dehydrogenase, p38 and JAK inhibitors in the rat adjuvant-induced arthritis model: a translational study, Br J Pharmacol, 166 (2012) 1320-1332.

[24] T.H. Page, J.J. Turner, A.C. Brown, E.M. Timms, J.J. Inglis, F.M. Brennan, B.M. Foxwell, K.P. Ray, M. Feldmann, Nonsteroidal anti-inflammatory drugs increase TNF production in rheumatoid synovial membrane cultures and whole blood, J Immunol, 185 (2010) 3694-3701.

[25] W. van Eden, J.P. Wagenaar-Hilbers, M.H. Wauben, Adjuvant arthritis in the rat, Curr Protoc Immunol, Chapter 15 (2001) Unit 15.14.

[26] P.P. Bradley, R.D. Christensen, G. Rothstein, Cellular and extracellular myeloperoxidase in pyogenic inflammation, Blood, 60 (1982) 618-622.

[27] K. Hoshino, O. Takeuchi, T. Kawai, H. Sanjo, T. Ogawa, Y. Takeda, K. Takeda, S. Akira, Cutting edge: Toll-like receptor 4 (TLR4)-deficient mice are hyporesponsive to lipopolysaccharide: evidence for TLR4 as the Lps gene product, J Immunol, 162 (1999) 3749-3752.

[28] Y.H. Nong, R.G. Titus, J.M. Ribeiro, H.G. Remold, Peptides encoded by the calcitonin gene inhibit macrophage function, J Immunol, 143 (1989) 45-49.

[29] Y. Feng, Y. Tang, J. Guo, X. Wang, Inhibition of LPS-induced TNF-alpha production by calcitonin gene-related peptide (CGRP) in cultured mouse peritoneal macrophages, Life Sci, 61 (1997) Pl 281-287.

[30] L.C. Davies, M. Rosas, P.J. Smith, D.J. Fraser, S.A. Jones, P.R. Taylor, A quantifiable proliferative burst of tissue macrophages restores homeostatic macrophage populations after acute inflammation, Eur J Immunol, 41 (2011) 2155-2164.

[31] A. Cassado Ados, J.A. de Albuquerque, L.R. Sardinha, L. Buzzo Cde, L. Faustino, R. Nascimento, E.E. Ghosn, M.R. Lima, J.M. Alvarez, K.R. Bortoluci, Cellular renewal and improvement of local cell effector activity in peritoneal cavity in response to infectious stimuli, PloS one, 6 (2011) e22141.

[32] A. Cassado Ados, M.R. D'Imperio Lima, K.R. Bortoluci, Revisiting mouse peritoneal macrophages: heterogeneity, development, and function, Front Immunol, 6 (2015) 225.

[33] Y. Okabe, R. Medzhitov, Tissue-specific signals control reversible program of localization and functional polarization of macrophages, Cell, 157 (2014) 832-844.

[34] L. Jansky, P. Reymanova, J. Kopecky, Dynamics of cytokine production in human peripheral blood mononuclear cells stimulated by LPS, or infected by Borrelia, Physiol Res, 52 (2003) 593-598.

[35] G.H. Giambartolomei, V.A. Dennis, B.L. Lasater, M.T. Philipp, Induction of pro-and anti-inflammatory cytokines by Borrelia burgdorferi lipoproteins in monocytes is mediated by CD14, Infect Immun, 67 (1999) 140-147.

[36] A. Ngkelo, K. Meja, M. Yeadon, I. Adcock, P.A. Kirkham, LPS induced inflammatory responses in human peripheral blood mononuclear cells is mediated through NOX4 and Gia dependent PI-3kinase signalling, J Inflamm (Lond), 9 (2012) 1-1.

[37] J.C. Chow, D.W. Young, D.T. Golenbock, W.J. Christ, F. Gusovsky, Toll-like receptor-4 mediates lipopolysaccharide-induced signal transduction, J Biol Chem, 274 (1999) 10689-10692.

[38] J. Willis, M. Kendall, R. Flinn, D. Thornhill, P. Welling, The pharmacokinetics of diclofenac sodium following intravenous and oral administration, Eur J Clin Pharmacol, 16 (1979) 405-410.

[39] F. Turesin, P. Del Soldato, J.L. Wallace, Enhanced anti-inflammatory potency of a nitric oxide-releasing prednisolone derivative in the rat, Br J Pharmacol, 139 (2003) 966-972.

[40] J.L. Masferrer, B.S. Zweifel, P.T. Manning, S.D. Hauser, K.M. Leahy, W.G. Smith, P.C. Isakson, K. Seibert, Selective inhibition of inducible cyclooxygenase 2 in vivo is antiinflammatory and nonulcerogenic, Proc Natl Acad Sci U S A, 91 (1994) 3228-3232.

[41] T. Wu, T. Chou, Y. Ding, M. Li, Stimulation of TNF-alpha, IL-1beta and nitrite release from mouse cultured spleen cells and lavaged peritoneal cells by mastoparan M., Immunol Cell Biol, 77 (1999) 476-482.

[42] T. Sandstrom, L. Bjermer, R. Rylander, Lipopolysaccharide (LPS) inhalation in healthy subjects increases neutrophils, lymphocytes and fibronectin levels in bronchoalveolar lavage fluid, Eur Respir J, 5 (1992) 992-996.

[43] A.M. Bendele, Animal models of rheumatoid arthritis, J Musculoskelet Neuronal Interact, 1 (2001) 377-385.

[44] T. Hamada, N. Arima, M. Shindo, K. Sugama, Y. Sasaguri, Suppression of adjuvant arthritis of rats by a novel matrix metalloproteinase-inhibitor, Br J Pharmacol, 131 (2000) 1513-1520.